Identification of Potential Predators for Asari Clam *Ruditapes philippinarum* Using Time-lapse Camera Observations

Naoaki TEZUKA[1]*, Yoshitake TAKADA[2], Toshihiro SHIGETA[1] and Motoharu UCHIDA[1]

[1] National Research Institute of Fisheries and Environment of Inland Sea, Japan Fisheries Research and Education Agency, Hatsukaichi, Japan
[2] Japan Sea National Fisheries Research Institute, Japan Fisheries Research and Education Agency, Niigata, Japan

Abstract

Predation is considered a significant factor contributing to the recently observed low survival rates of asari clam (*Ruditapes philippinarum*) in Japan. Longheaded eagle ray, blackhead seabream, portunid crabs, predatory gastropods, and ducks are suggested as potential predators; however, the relative significance of these predators has yet to be evaluated. In this study, we conducted 31 single-day time-lapse camera observation trials during summer at 28 stations within 12 habitats of the asari clam in Japan (ranging from temperate to subarctic regions) to determine the relative abundance of predators in each habitat. And in a trial at the Nakatsu tidal flat in southwestern Japan, where a previous study observed a low survival rate of the asari clam, the absolute abundances of different predator taxa were estimated by quantifying the underwater visibility and visible area in images. The blackhead seabream (*Acanthopagrus schlegelii*), a known temperate subtropical species, was identified as the most frequently observed predator. *A. schlegelii* was widely observed in 8 of the 12 habitats in the southwestern to central regions of Japan. The longheaded eagle ray was not observed, and portunid crabs and predatory gastropods were few in this study. At Nakatsu, a maximum of 39 individuals of *A. schlegelii* were observed in a single trial (via single-day images captured every 2 min.), indicating the significance of this predator relative to asari clam mortality at this site. *A. schlegelii* appeared on the tidal flat during high tide, and its hourly mean abundance exceeded 20 ind./100 m^2 during high tide after dawn. Rising seawater temperatures along Japan's coast might increase the predation risk for asari clam posed by temperate-to-subtropical risk species.

Discipline: Fisheries
Additional key words: fish species composition, global warming, underwater observation

Introduction

The asari clam *Ruditapes philippinarum* (also known as Manila clam) is a common inhabitant of estuarine tidal flats in the temperate to subarctic regions of Japan. Asari clams are commercially harvested and constitute an important local fishery resource. However, the fishery production of asari clam has largely decreased over the past 30 years, especially in the southwestern to central parts of Japan (Toba et al. 2007, Tamaki et al. 2008, Tezuka et al. 2012, Toba 2017, Toba et al. 2020). Observed annual survival rates of asari clam post-settlement were as low as 0%-15% in the Nakatsu tidal flat in southwestern Japan, known as a population-collapsed habitat for the clams (Tezuka et al. 2012), and predation was considered a significant contributor to asari clam mortality (Tezuka et al. 2014). Asari clam production is becoming increasingly difficult, particularly in southwestern Japan, without adequate predator-preventive measures such as netting and caging.

Certain species of fish, portunid crabs, predatory gastropods, and ducks are known predators of the asari clam (Kimura 2005, Lewis et al. 2007, Sato et al. 2012, Shigeta & Usuki 2012, Takahashi et al. 2016, Sun et al. 2017). In recent years, the longheaded eagle ray (Yamaguchi et al. 2005, Ito & Hirakawa 2009) and

blackhead seabream (Shigeta & Usuki 2012) have been recognized as significant predators of the clam in southwestern Japan, along with portunid crabs in some areas (Kimura 2005, Takahashi et al. 2016). And a growing population of predatory gastropods has been widely reported from southwestern (Hirayama et al. 1996), central (Segawa & Hattori 1997, Shibata & Kawanishi 1999, Okamoto 2000), and northeastern areas of Japan (Sato et al. 2012). However, the relative abundance of different predator species and the significance of each for asari clam mortality have yet to be evaluated.

Underwater camera observations can be used to determine the relative abundance of different predators in asari clam habitats. The impact of each predator species can be expressed as the product of the observed abundance and individual predation rate. The individual predation rate can be measured by other means (e.g., tank experiments), depending on the species (prey preference) and body size. Predators observed more frequently would have a greater impact than rarely observed predators, given the same individual predation rate. Predators with a higher individual predation rate would have a greater impact than those with a lower rate, given the same frequencies of observation. In this study, we conducted single-day, time-lapse camera observation trials within 12 habitats of asari clam along the coast of Japan in order to estimate the predator composition in each habitat. Despite the limited trials, the results will aid future efforts in more precisely estimating the impact of the observed predators on asari clam mortality.

Methods

1. Underwater camera observations

A total of 31 single-day, time-lapse camera observation trials were conducted at 28 stations within 12 asari clam habitats in Japan, ranging from temperate to subarctic regions. Figure 1 shows a map of the locations of the 12 habitats and 28 stations. The stations were set in intertidal areas mainly inhabited by the asari clam, except at Hamana, where the clams (and thus the stations) were mainly distributed in the subtidal area. Trials were conducted on days during spring tide in summer (July to September), from 2013 to 2017. Table 1 lists the dates of each trial. During several of the trials (see Table 1), the water temperature, water level, and salinity were recorded every 10 min., using a HOBO U20 water level data logger (Onset Corp.) and a Compact–CT data logger (JFE Advantech Co. Ltd.).

For each trial, a time-lapse camera with waterproof housing and affixed to a plastic pole was installed at the station during low tide in the daytime. The camera was set in portrait (vertical) orientation at approximately 20 cm-25 cm above the seabed, with the view aimed approximately 5°-10° downward (Fig. 2). Still images were captured every 5 min. (in 2013) or every 2 min. (all other years) until the camera was retrieved the following day during low tide. A built-in automatic flash was used under low-light conditions.

One of the following camera models was deployed in each trial: Optio WG-1 or WG-20 (RICOH Co. Ltd.), or Exilim ZS35 or ZS27 (CASIO Co. Ltd.). Table 2 lists the focal length, image sensor size, and underwater field of view of both camera models. Assuming that underwater visibility was 2.5 m, although it actually varied, the visible area depicted in the image within a 2.5-m distance from the camera was 2.0 m^2 for the Optio, and 2.1 m^2 for the Exilim. In a trial at the Nakatsu tidal flat (NK4-15), plastic poles marking distances of 1 m, 2 m and 3 m from the camera were installed to roughly estimate underwater visibility for each time-lapse captured image.

2. Data analysis

The captured images were displayed on a desktop PC monitor (21.5″, full HD) in a laboratory, using the Parapara viewer, a HTML image viewer with a note-taking function (Tezuka 2018). All individual fish, crabs, and gastropods within each image were identified to the lowest possible taxonomic level and enumerated. Migratory ducks that appear in winter were absent as our trials were conducted during summer. Unidentified juvenile fish, small-sized crustaceans (e.g., hermit crabs and *Hemigrapsus* spp.), and small-sized gastropods (e.g., *Batillaria* spp.) were not included in the enumeration. All individuals in an image were counted regardless of being identical between images. However, in a trial at Hamana (HM2-16), a predatory gastropod (*Neverita didyma*) was observed in front of the camera but did not move during the trial, and thus was counted as one individual per trial.

To determine species composition, the number of individuals per trial was calculated for each habitat as follows, and then graphically depicted (see Results, Fig. 4):

$$\text{Number of individuals per trial (ind. / trial)} = \frac{\sum_{i=1}^{n} Ni}{n}$$

where n is the number of trials conducted in the habitat, and Ni is the number of individuals in trial i. Given the potential for overestimation, Gobiidae species were excluded due to their low movement frequency (i.e., often remaining stationary in front of the camera) and as their small body size would have a lesser effect on the benthic assemblages. Unidentified species were also excluded.
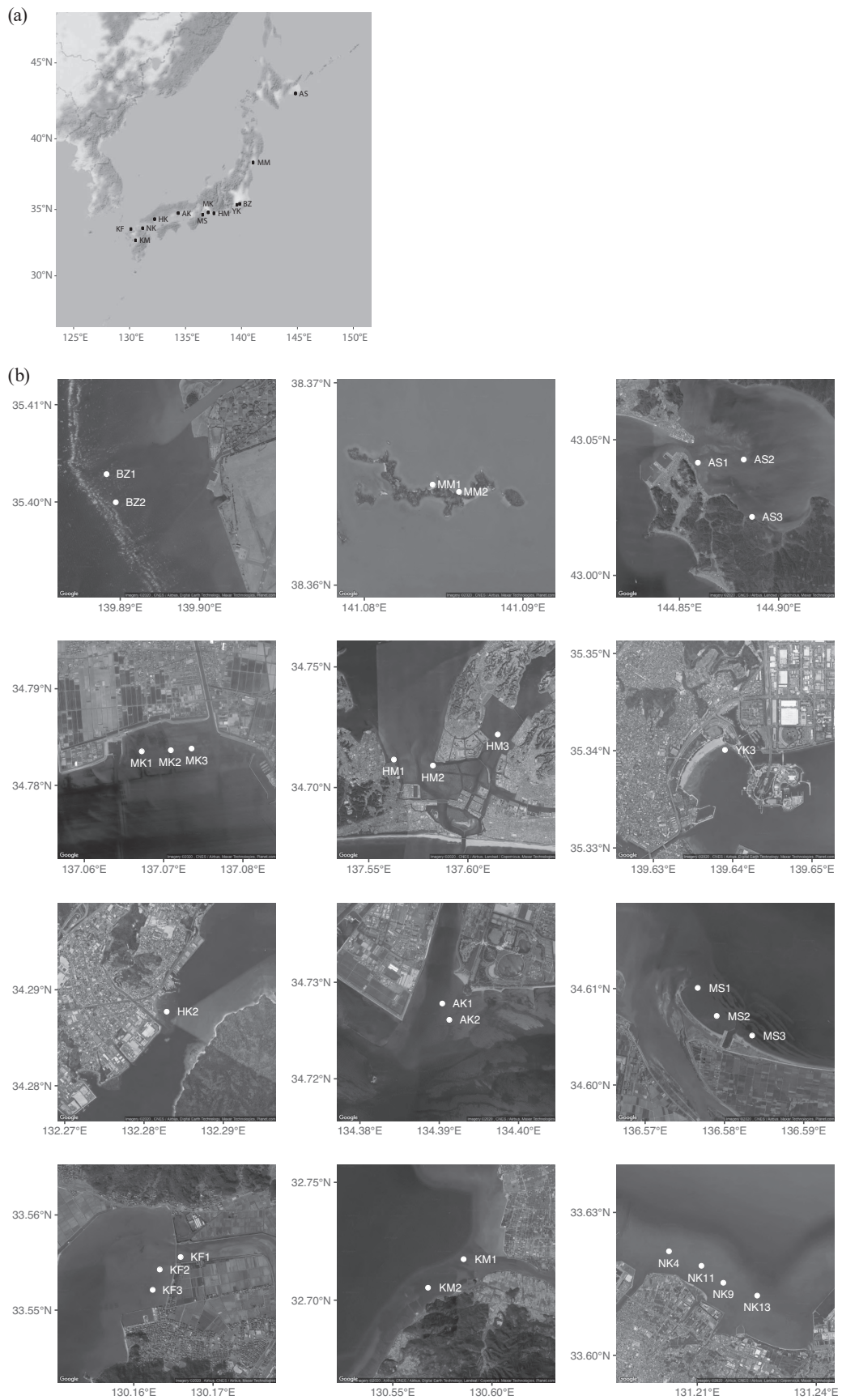
Fig. 1. Map showing (a) 12 habitats and (b) 28 stations where time-lapse camera observation trials were conducted

Table 1. List of stations and date of each time-lapse camera observation trial

Trial ID	Habitat name, Pref.	Date	Station	Tidal range (m)	Water temperature range (°C)	Salinity range
AS1-16	Akkeshi, Hokkaido	Jul. 20-21, 2016	AS1	0-0.6	14.1-16.1	27.0-31.0
AS2-16		Jul. 20-21, 2016	AS2			
AS3-16		Jul. 20-21, 2016	AS3			
MM1-17	Matsushima, Miyagi	Jul. 25-26, 2017	MM1	0-1.3 (*1)	24.8-27.9 (*1)	
MM2-17		Jul. 25-26, 2017	MM2			
BZ1-14	Banzu, Chiba	Aug. 26-27, 2014	BZ1	0-1.4	23.1-27.1	24.9-32.4
BZ2-14		Aug. 26-27, 2014	BZ2			
YK3-13	Yokohama, Kanagawa	Aug. 20-21, 2013	YK3			
MK2-13	Mikawa, Aichi	Sep. 3-4, 2013	MK2			
MK1-14		Jul. 29-30, 2014	MK1	0-1.8	26.6-29.8	29.6-31.9
MK3-14		Jul. 29-30, 2014	MK3			
AK1-13	Ako, Hyogo	Aug. 7-8, 2013	AK1			
AK1-14		Jul. 22-23, 2014	AK1	0.4-1.8	27.0-31.3	15.6-31.5
AK2-14		Jul. 22-23, 2014	AK2			
HM2-16	Hamana, Shizuoka	Aug. 3-4, 2016	HM2	0.9-1.5 (*2)	27.5-30.6 (*2)	
HM3-16		Aug. 3-4, 2016	HM3			
MS1-15	Matsusaka, Mie	Sep. 15-16, 2015	MS1	0-1.7	23.9-25.9	17.0-25.2
MS2-15		Sep. 15-16, 2015	MS2			
MS3-15		Sep. 15-16, 2015	MS3			
HK2-13	Hamakebo, Hiroshima	Sep. 17-18, 2013	HK2			
NK4-13	Nakatsu, Oita	Sep. 10-11, 2013	NK4	0-2.1	26.5-29.6	
NK4-14		Aug. 11-12, 2014	NK4	0-2.9	25.5-29.1	26.0-30.4
NK9-14		Aug. 11-12, 2014	NK9			
NK4-15		Jul. 28-29, 2015	NK4	0-2.1	26.5-34.5	23.7-31.0
NK11-15		Jul. 28-29, 2015	NK11			
NK13-15		Jul. 28-29, 2015	NK13			
KF1-15	Kafuri, Fukuoka	Sep. 29-30, 2015	KF1	0-1.6	21.9-22.8	27.4-33.4
KF2-15		Sep. 29-30, 2015	KF2			
KF3-15		Sep. 29-30, 2015	KF3			
KM1-14	Uto, Kumamoto	Sep. 9-10, 2014	KM1	0-3.4	25.2-27.9	16.9-30.7
KM2-14		Sep. 9-10, 2014	KM2			

(*1) Tidal range at MM1-17 was estimated from the tide table at a nearby site. Temperature was recorded by DS18B20.
(*2) Tidal range and water temperature was recorded at HM1 (see Fig. 1).

Fig. 2. The time-lapse underwater cameras used in single-day observation trials in intertidal habitats

For a trial at Nakatsu (NK4-15) where underwater visibility was estimated, the number of individuals was accumulated every hour (for every 30 images), and hourly differences in the number of individuals were graphically presented along with temporal changes in the water temperature, water level, and underwater visibility (see Results, Fig. 5).

The hourly and daily mean abundances were also calculated for the trial at Nakatsu (NK4-15) as follows:

$$\text{Mean abundance (ind.} / \text{m}^2) = \frac{\sum_{i=1}^{n} Ni / Ai}{n}$$

where n is the number of images, Ni is the number of individuals in image i, and Ai is the visible area in image i. Hourly mean abundance was calculated with $n = 30$ images (photographed every 2 min. for 1 h). Daily mean abundance was calculated as $n = 720$ (every 2 min. for 1 day), with the number of individuals during low tide

Table 2. Focal length, image sensor size and underwater field of view for the Optio and Exilim cameras used in this study

Camera model	Focal length	Image sensor size	Horizontal underwater FOV	Vertical underwater FOV
Optio WG-1or 20 (Richo, Co. Ltd.)	5.0 mm	1/2.3″	36.4°	47.5°
Exilim ZS27 or 35 (CASIO Co. Ltd.)	4.6 mm	1/2.3″	39.3°	51.2°

(water level zero) set at $Ni = 0$. By using the mean abundances, differences in the numbers of individuals photographed under different visibility conditions could be compared (e.g., abundance of diurnal vs. nocturnal species).

The visible area in image i was calculated as:

$$Ai(\text{m}^2) = \pi \times Vi^2 \times \frac{\theta}{360}$$

where Vi is the underwater visibility (m) in image i, π is the circular constant, and θ is the underwater field of view (°) of the camera.

The underwater field of view was calculated as:

$$\theta(°) = 2 \times \arctan\left(\frac{L}{2 \times f \times R}\right) \times \frac{180}{\pi}$$

where L is the size of the image sensor (vertical size of a 1/2.3″ image sensor, with $L = 4.4$ mm used in this study), f is the focal length of the camera ($f = 5.0$ mm for the Optio), and R is the refractive index of seawater ($R = 1.34$). Assuming underwater visibility at 1 m, 2 m or 3 m, and an underwater field of view of the camera at 36.4°, the visible area in an image was calculated as 0.32, 1.3 or 2.9 m^2, respectively. These analyses were conducted with R (R Core Team 2019).

Results

A total of 23 taxonomic groups was identified in the observation trials. Figure 3 shows examples of the captured images; Table 3 lists the number of individuals in each taxa identified in each trial. Gobiidae was the most frequently observed taxa, and these fishes were found abundantly at subtidal stations (Hamana: HM2 and HM3) and near subtidal stations (Ako: AK1; Kafuri: KF3). However, their observed abundance may have been overestimated as gobiids move infrequently and individuals often remained positioned in front of the camera once they appeared. The blackhead seabream (*Acanthopagrus schlegelii*) was identified as the second-most frequently present, followed by the ponyfish (*Nuchequula nuchalis)*, flathead grey mullet (*Mugil cephalus*), Japanese seabass (*Lateolabrax japonicus*), red stingray (*Hemitrygon akajei*), and pufferfish (*Tetraodontidae*), among others. Among known predators of the asari clam, *A. schlegelii* was identified as the most

abundant, with a maximum of 39 individuals recorded in a single trial (at Nakatsu, NK4-15). Though portunid crabs (*Portunus* spp.) and predatory gastropods (*Neverita didyma*, *Laguncula pulchella*, and *Rapana venosa*) were identified in some trials, the numbers of individuals were very few. The longheaded eagle ray (*Aetobatus flagellum*) was not observed in this study.

The total numbers of individuals largely varied among the trials. Spatial differences were observed even among stations on the same day within the same habitat. For example, at the Nakatsu tidal flat in 2015, the total number of individuals was 83 at NK4-15, which was more than 10-times greater than at other stations on the same day (i.e., 7 individuals at NK11-15, 6 individuals at NK13-15). Similar large spatial variation was observed between two stations at Ako in 2014 (AK1-14, AK2-14), and among three stations at Kafuri in 2015 (KF1-15, KF2-15, and KF3-15). Greater numbers of individuals were observed at the near-river-mouth stations at Nakatsu (NK4-15) and Ako (AK1-14). Temporal differences were also observed between trials conducted in different years at the same station. At Nakatsu, where trials were conducted in 2014 and 2015 (NK4-14 and NK4-15), the numbers of individuals differed approximately five times between the years, with 16 individuals counted at NK4-14 and 83 at NK4-15. In several trials, the total number of enumerated individuals was few partly due to low underwater visibility (e.g., at silty sites). In particular, the trials at Kumamoto (KM), Matsusaka (MS), Matsushima (MM), Mikawa (MK), and some at Akkeshi (AS3-16) and Nakatsu (NK9-14, NK13-15) occurred under low visibility conditions.

Figure 4 shows the numbers of individuals per trial (i.e., species composition excluding Gobiidae and unidentified species) for each habitat. Species composition was not adequately determined for Matsuhima (MM), Matsusaka (MS), and Kumamoto (KM) as few individuals contributed to the total numbers, partly due to low visibility at those habitats.

Acanthopagrus schlegelii was the most-commonly found species, identified at 8 of the 12 habitats, which excluded the sites in northern Japan (Akkeshi and Matsushima) and along the Ariake Sea (Kumamoto). In Tokyo Bay, *A. schlegelii* was identified at Yokohama (YK) but not at Banzu (BZ), although yellowfin seabream (*A. latus*) was identified at BZ. *Mugil cephalus* was the
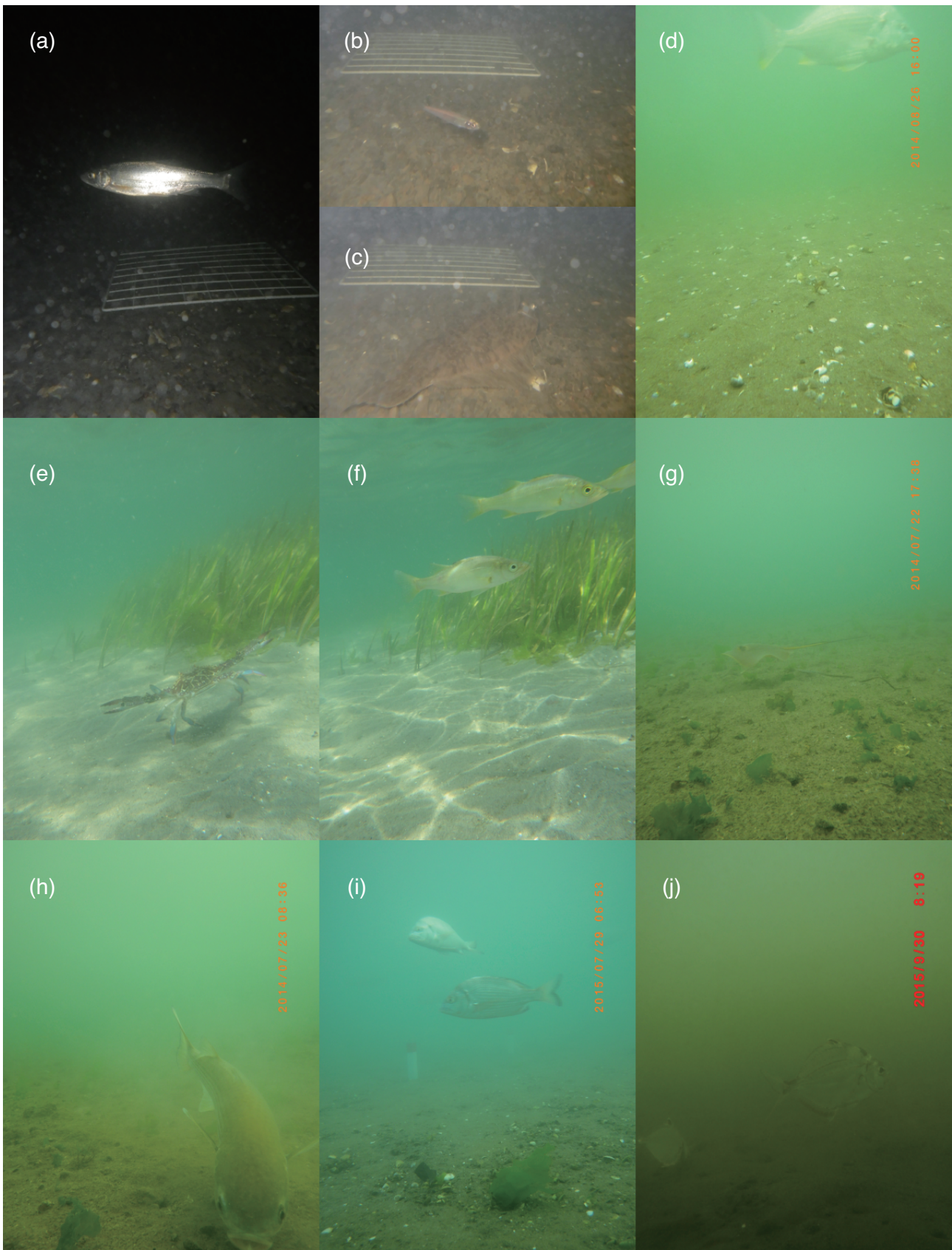
Fig. 3. Examples of images captured by the time-lapse underwater cameras
(a) *Tribolodon* sp., (b) *Hypomesus* sp., (c) *Pseudopleuronectes* sp., (d) *Acanthopagrus latus*, (e) *Portunus pelagicus*, (f) *Lateolabrax japonicus*, (g) *Hemitrygon akajei*, (h) *Mugil cephalus*, (i) *Acanthopagrus schlegelii*, and (j) *Nuchequula nuchalis*

Table 3. Number of individuals and the species groups identified by the time-lapse camera observation trials

Trial ID	Go	As	Nn	Mc	Lj	Ha	Te	Hp	Hy	Pl	Pc	Ps	Se	Ro	Al	Rv	Re	Nd	Lp	An	Tr	Pr	Af	Un	Total
AS1-16	1	0	0	0	0	0	0	0	0	0	0	0	0	0	0	0	0	0	0	0	2	0	0	7	10
AS2-16	0	0	0	0	0	0	0	0	6	0	0	5	0	0	0	0	0	0	0	0	0	0	0	1	12
AS3-16	0	0	0	0	0	0	0	0	0	0	0	0	0	0	0	0	0	0	0	0	0	0	0	2	2
MM1-17	17	0	0	0	0	0	0	0	0	0	0	0	0	0	0	0	0	0	0	0	0	0	0	2	19
MM2-17	2	0	0	0	0	0	0	0	0	0	0	0	0	0	0	0	0	0	0	0	0	0	0	0	2
BZ1-14	7	0	0	2	0	3	0	0	0	0	0	0	0	0	0	0	0	1	0	0	0	0	0	9	22
BZ2-14	0	0	0	0	0	6	0	0	0	0	0	0	0	0	1	3	0	0	0	0	0	0	0	4	14
YK3-13	0	2	0	0	0	1	1	0	0	0	0	0	0	3	0	0	0	0	0	0	0	0	1	4	12
MK2-13	0	9	1	0	0	0	0	0	0	0	0	0	0	0	0	0	0	0	0	0	0	0	0	1	11
MK1-14	3	0	0	1	0	0	0	0	0	0	0	0	0	0	0	0	0	0	0	0	0	0	0	2	6
MK3-14	1	0	0	5	1	0	0	0	0	0	0	0	0	0	0	0	0	0	0	0	0	0	0	2	9
AK1-13	24	2	0	2	0	0	0	0	0	0	0	0	0	0	0	0	0	0	0	0	0	0	0	6	34
AK1-14	29	12	6	19	0	4	0	0	0	0	0	0	0	0	2	0	1	0	0	0	0	0	0	22	95
AK2-14	2	1	0	0	0	0	0	0	0	0	5	0	0	0	0	0	0	0	0	0	0	0	0	2	10
HM2-16	29	2	0	2	22	0	0	0	0	0	0	0	0	0	0	0	1	1	0	0	0	2	0	22	81
HM3-16	11	2	0	0	0	0	0	0	0	0	0	0	0	0	0	0	0	0	0	0	0	0	0	2	15
MS1-15	0	0	0	0	0	0	0	0	0	0	0	0	0	0	0	0	0	0	0	0	0	0	0	0	0
MS2-15	1	1	0	0	0	0	0	0	0	0	0	0	0	0	0	0	0	0	0	0	0	0	0	0	2
MS3-15	0	0	0	0	0	2	0	0	0	0	0	0	0	0	0	0	0	0	0	0	0	0	0	1	3
HK2-13	1	3	0	2	0	0	8	8	0	0	0	0	4	0	0	0	0	0	0	0	0	0	0	16	42
NK4-13	2	4	0	0	1	0	0	0	0	0	0	0	0	0	0	0	0	0	0	0	0	0	0	0	7
NK4-14	3	3	0	0	0	3	0	0	0	0	0	0	0	0	0	0	0	0	0	0	0	0	0	7	16
NK9-14	0	0	0	0	0	0	0	0	0	0	0	0	0	0	0	0	0	0	0	0	0	0	0	1	83
NK4-15	0	39	13	6	5	1	0	0	0	0	0	5	0	0	0	0	0	0	0	0	0	0	0	14	1
NK11-15	0	3	0	0	0	0	0	0	0	0	0	0	0	0	0	0	0	0	0	0	0	0	0	4	7
NK13-15	0	1	0	1	0	0	0	0	0	0	0	0	0	0	0	0	0	0	0	0	0	0	0	4	6
KF1-15	1	0	1	0	1	0	0	0	0	0	0	0	0	0	0	0	0	0	0	0	0	0	0	0	3
KF2-15	3	2	15	1	0	0	1	0	0	0	0	0	0	0	0	0	0	0	0	2	0	0	0	1	25
KF3-15	72	1	18	0	0	0	0	0	0	0	0	0	0	0	0	0	0	0	0	0	0	0	0	5	96
KM1-14	4	0	0	0	0	0	0	0	0	0	0	0	0	0	0	0	0	0	0	0	0	0	0	1	5
KM2-14	1	0	0	0	0	0	0	0	0	0	0	0	0	0	0	0	0	0	0	0	2	0	0	0	3
Total	214	87	54	41	30	20	10	8	6	5	5	5	4	3	3	3	2	2	2	2	2	2	1	142	653

Abbreviations are as follows. Go: Gobiidae,   As: *Acanthopagrus schlegelii*, Nn: *Nuchequula nuchalis*, Mc: *Mugil cephalus*, Lj : *Lateolabrax japonicus*, Ha: *Hemitrygon akajei*, Te: *Tetraodontidae*, Hp: *Halichoeres poecilopterus*, Hy: *Hypomesus* sp., Pl : *Pleuronectidae*, Pc: *Plectorhinchus cinctus*, Ps: *Pseudopleuronectes* spp., Se: *Sebastes* sp., Ro: *Rhyncopelate oxyrhynchus*, Al : *Acanthopagrus latus*, Rv: *Rapana venosa*, Re: *Rudarius ercodes*, Nd: *Neverita didyma*, Lp: *Laguncula pulchella*, An: *Anguilla* sp., Tr: *Tribolodon* sp., Po: *Portunus* sp., Af: Anguilliformes, and Un: Unidentified.

second-most-commonly found species, being identified at 7 of the habitats. Similar to *A. schlegelii*, *M. cephalus* was not observed at the sites in northern Japan (AS and MM) and on the Ariake Sea (KM). *Hemitrygon akajei* was the third-most-commonly found species, identified at 5 of the habitats, and was the dominant species at Banzu (BZ) in Tokyo Bay. Also commonly identified were *N. nuchalis* and *L. japonicus* (both species at 4 habitats) and *Tetraodontidae* (at three habitats). *Nuchequula nuchalis* was dominant at Kafuri (KF), *L. japonicus* at Hamana (HM), and *Tetraodontidae* at Hamakebo (HK).

Figure 5 shows hourly changes in the numbers of individuals with temporal changes in the water temperature, water level, and underwater visibility for a trial at Nakatsu (NK4-15). Underwater visibility varied with the water level and light intensity (day and night), and was < 2 m during low tide to flood tide, and 2 m - 3 m during high tide to ebb tide. Visibility reached 3 m during high tide in the daytime, but not during high tide at nighttime. In this particular trial, a total of 39 individuals of *A. schlegelii* was observed during high tide, particularly during the second high tide after dawn. Few *A. schlegelii* were observed at night, whereas *N. nuchalis* and *L. japonicus* were observed more often at night. Figure 6 shows the hourly mean abundances. The hourly mean abundance of *A. schlegelii* exceeded 20 ind./100 m^2 during the second high tide after dawn, and its daily mean abundance was calculated as 3.7 ind./100 m^2. Table 4 lists the daily mean abundance of the other species.
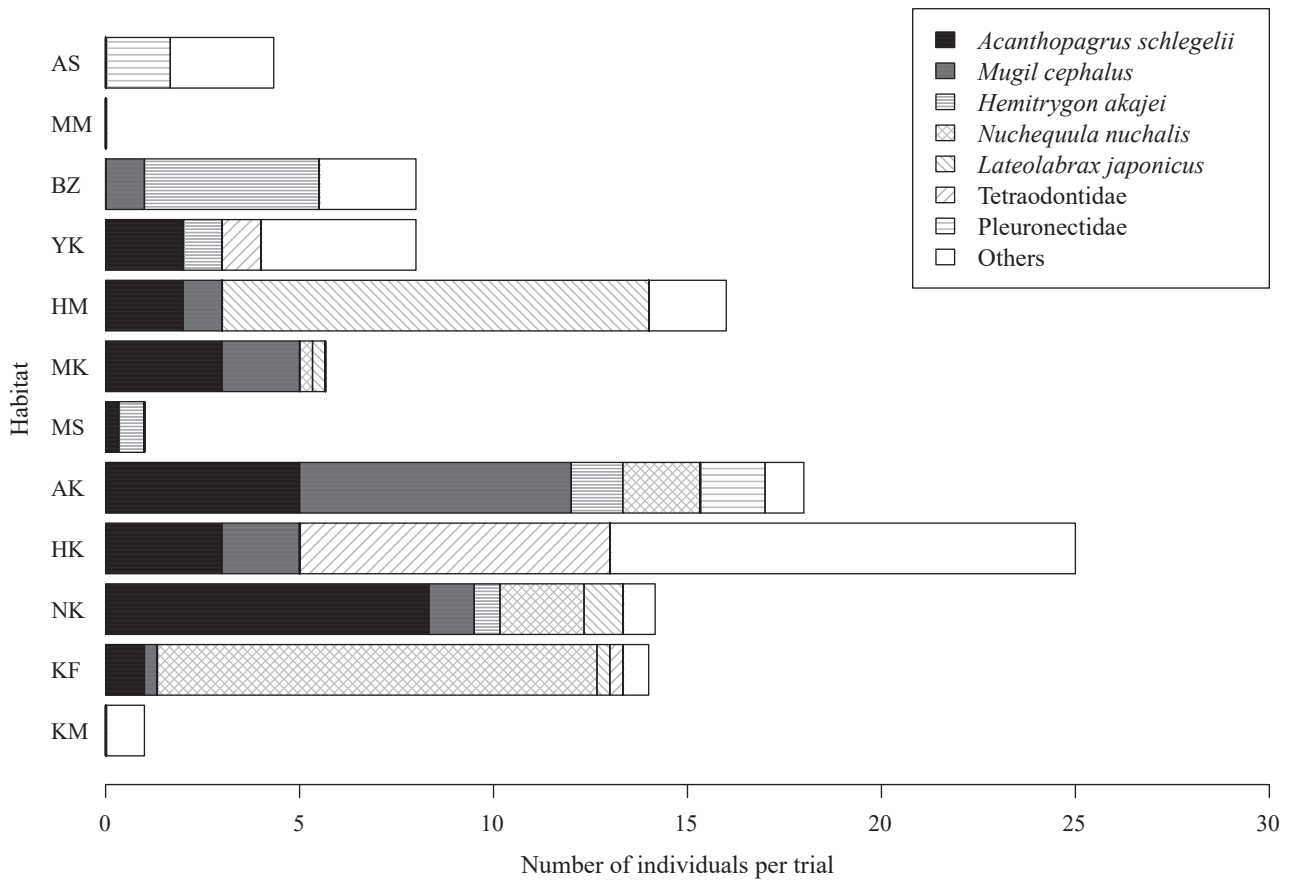
Fig. 4. The number of individuals per trial for each habitat
(excluding data for Gobiidae and unidentified species)
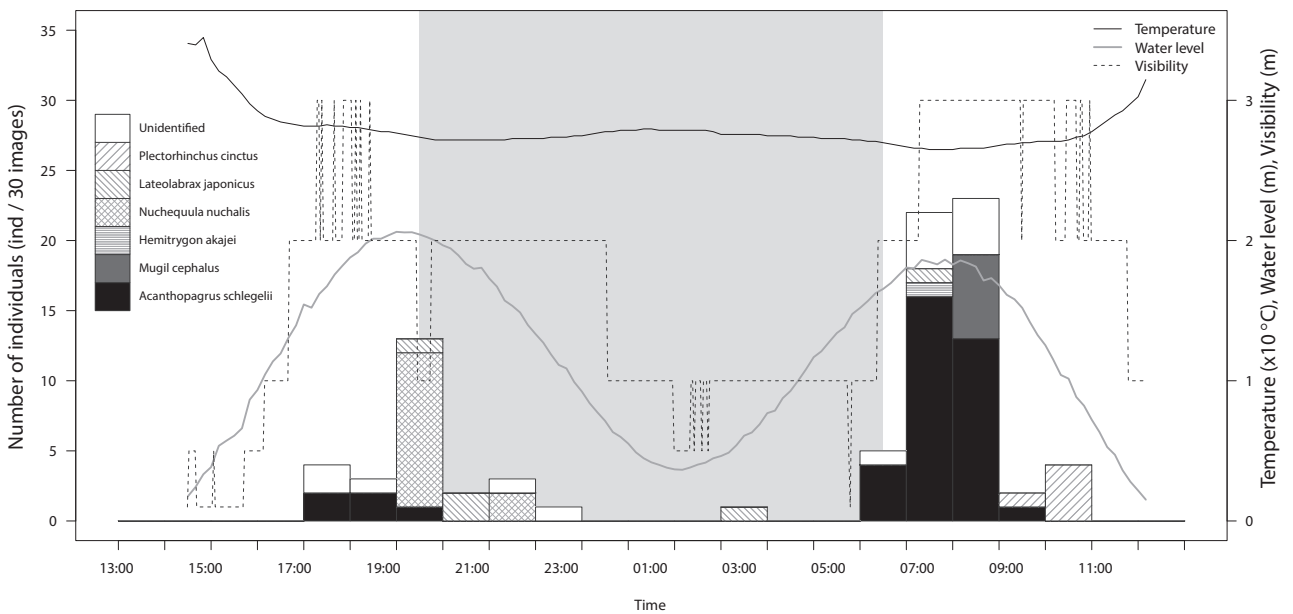
Fig. 5. Hourly changes in the number of individuals, along with temporal changes in water temperature, water level, and underwater visibility, in a trial at Nakatsu tidal flat (NK4-15)
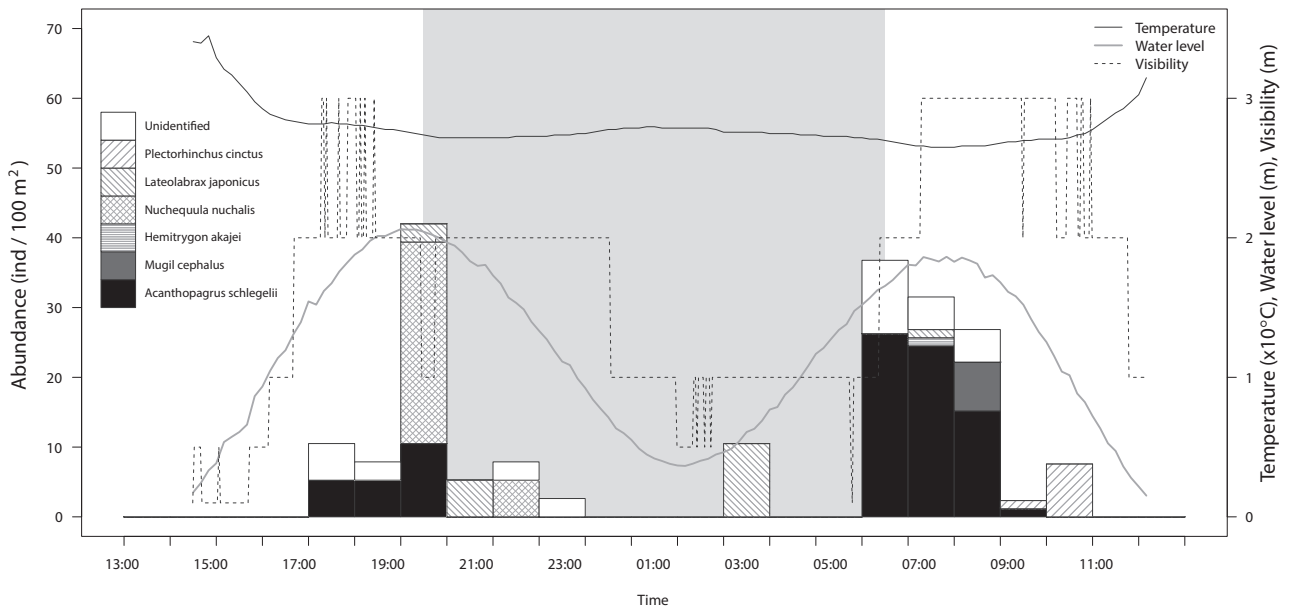
Fig. 6. Hourly mean abundances relative to changes in water temperature, water level, and underwater visibility, in a trial at Nakatsu tidal flat (NK4-15)

Table 4. Daily mean abundances of the taxa identified at the Nakatsu tidal flat, NK4-15

Species	*Acanthopagrus shelegelii*	*Mugil cephalus*	*Hemitrygon akajei*	*Nuchequula nuchalis*	*Lateolabrax japonicus*	*Plectorhinchus cinctus*	Unidentified
Abundance (ind./100 m²)	3.67	0.29	0.05	1.42	0.81	0.36	1.37

Discussion

Our underwater camera observations effectively revealed the species composition of fishes that migrated into the intertidal zone during high tide. However, several complications of this approach became evident. First, observed variations in the numbers of individuals of the fishes related not only to spatiotemporal differences in their abundance, but also coincided with underwater visibility. In several trials under low-visibility conditions, few individuals were recorded. Furthermore, the difference in underwater visibility between day and night would cause an underestimation of nocturnal species. Second, the observed abundance of species that have low movement frequency or ability (e.g., Gobiidae, predatory gastropods) would entail a large observation error. These species would be overestimated if remaining in front of the camera for a long time and vice-versa. However, this error can be reduced by conducting a sufficient number of observations. Third, body size would affect the abundance estimation. Small-sized species (e.g., Gobiidae, predatory gastropods) could be underestimated as they were generally more difficult to find in the images and when the individuals were located farther from the camera. Fourth, rare species might not have been detected due to the limited frequency of the trials. Longer recording times or the use of multiple camera observations accompanied by visibility estimates are required to more precisely evaluate the species composition and abundance.

Despite these aspects, the dominant taxa within habitats of the asari clam were identified as follows: Gobiidae, *Acanthopagrus schlegelii*, *Mugil cephalus*, *Hemitrygon akajei*, *Lateolabrax japonicus*, *Nuchequula nuchalis*, and *Tetraodontidae*. Except for *L. japonicus*, these fishes all prey on benthic infauna, and thus will impact the infaunal assemblage. Among them, *A. schlegelii* and *Tetraodontidae* are known predators of the asari clam (Shigeta & Usuki 2012). Though *H. akajei* reportedly fed on asari clams (Kodama & Taino 2014, Suzuki et al. 2018), bivalves are generally not considered a major food of that species (Kanazawa 2003). *Nuchequula nuchalis* is known as a benthic feeder, including the consumption of bivalves (Ochiai & Tanaka 1986). Among all these taxa, *A. schlegelii* would be the most significant predator, given its generally larger body size than that of tetraodontids and *N. nuchalis*. In a dietary analysis, asari clams accounted for 72.5% of the

93

stomach contents (wet weight) of *A. schlegelii* (sized 24.7-42.3 cm TL) (Shigeta & Usuki 2012), indicating a high individual predation rate on asari clams.

Acanthopagrus schlegelii were identified at 8 of the 12 habitats in southwestern to central Japan, indicating their predation on asari clams may be widespread and common. Especially at the Nakatsu tidal flat in southwestern Japan, where a previous study observed a low survival rate of asari clams (Tezuka et al. 2012), a maximum of 39 individuals of *A. schlegelii* was recorded in one trial, and abundance of this fish reached more than 20 ind./100 m^2 during high tide. Predation was considered a major cause of the clam's low survival rate in the tidal flat, as their survival improved after predator-preventive netting was installed (Tezuka et al. 2014). However, the previous study did not identify the predator species involved. The present study strongly suggests that predation by *A. schlegelii* is a significant cause of asari clam mortality at Nakatsu, and likely at other habitats where this fish was frequently identified.

Predator-preventive netting has become indispensable for the commercial production of asari clams, at least in southwestern Japan (Ito & Ogawa 1999, Taga et al. 2005, Saito et al. 2010, Tezuka et al. 2014, Izumikawa et al. 2015, Kodama & Taino 2018, Tsujino & Shigeta 2019). Rising seawater temperatures along Japan's coast (Japan Meteorological Agency 2019) may have increased the predation risk for asari clams by temperate-to-subtropical predators, as seen in macroalgal habitats along the coast where increases and expanding distributions of subtropical herbivorous fish have caused decreases in vegetation (Kumagai et al. 2018). The effect of *A. schlegelii* on the clam's mortality should be monitored and further examined in wider regions of Japan.

In contrast, the longheaded eagle ray was not identified, and the numbers of portunid crabs and predatory gastropods were few in this study, although these species have been suggested as significant predators of asari clams. The known distribution of longheaded eagle ray extends to southwestern Japan (Yamaguchi et al. 2005, Ito & Hirakawa 2009), including Nakatsu, Hamakebo, and Kumamoto. The results suggest that longheaded eagle rays are less frequent in the intertidal zone as compared with other predators, including *A. schlegelii*. The effect of the longheaded eagle ray on asari clam mortality would be lower than that of *A. schlegelii*, even though its individual predation rate was 10-times higher than that of *A. schlegelii* (Usuki et al. 2012) as its frequency of appearance would be less than 1/10. Furthermore, the rays might occur more commonly in subtidal areas than in intertidal areas, where our cameras were situated. The appearance frequency of the longheaded eagle ray should be determined over longer periods and at numerous sites to gauge its actual impact on the clam's mortality.

Portunid crabs and the predatory gastropods *Neverita didyma*, *Laguncula pulchella*, and *Rapana venosa* are widely distributed in Japan. However, these taxa might have been underestimated by our camera observations given their nocturnal nature (reduced visibility at night) and relatively small body sizes (difficult to identify farther from the camera). And if these taxa distribute more frequently at sites with lower visibility (e.g., silty habitat), they would have been underestimated due to smaller visible areas in the images. The abundance of these species and their probable effects on asari clam mortality thus require more precise estimations.

This study found that the abundance of migratory fishes varied spatiotemporally, with differences in abundances varying 5-10 times, which could not be explained by changes in underwater visibility alone. Greater numbers of individuals were observed near river-mouth sites at Nakatsu (NK4-15) and Ako (AK1-14). Tidal currents are faster at river mouths, and thus fish may use the current to enter an intertidal area. At those sites, bottom grain sizes were greater and benthic organisms including the asari clam were more abundant (Takada et al. 2020). The abundance of migratory fish may also relate to the abundance of prey. Temporal differences in fish abundance may be affected by differences in the water level relative to the tide, the timing of high tides (day or night), declines in salinity, and increased turbidity after rains. And as fish often form schools and migrate together, such behavior could cause both spatial and temporal variations in abundance. Future studies could employ camera observations that include estimations of underwater visibility to investigate the causes of spatiotemporal differences in fish abundance in intertidal habitats.

Camera methods have been increasingly used in aquatic research in recent years (Bett 2003, Mallet & Pelletier 2014). However, few studies have deployed underwater cameras in a tidal flat environment. The method employed in this study revealed the species composition of migratory predators of the asari clam, but the approach was compromised due to poor visibility conditions and the emergence of several other issues. The estimation of underwater visibility is necessary for comparing spatiotemporal differences in predator abundances, which varied largely in the tidal flat environment. An improved means of estimating underwater visibility is needed because accuracy will

affect the abundance calculation. Using a stereo or multi-lens camera apparatus may be applicable for estimating visibility as well as fish body sizes. Moreover, improved methods are needed to better identify and enumerate fish from numerous underwater images. Recent developments in the field of computer vision (i.e., image recognition using deep-learning) should assist with that (Siddiqui et al. 2018). Overall, underwater camera observations can help elucidate the current state of coastal ecological processes and changes.

Acknowledgements

References

Bett, B. J. (2003) Time-lapse photography in the deep sea. *J. Soc. Underwater Technol.*, **25**, 121-128.

Hirayama, I. et al. (1996) Predation of a shortneck clam by gastropod in the river mouth of Midori River. *Report of Kumamoto Prefectural Fisheries Research Center*, **3**, 12-17 [In Japanese].

Ito, R. & Hirakawa, C. (2009) Observation of stomach and intestinal contents to reveal the feeding habits of the longheaded eagle ray, *Aetobatus flagellum*, in the coastal waters of Southern Suo-Nada, Seto Inland Sea, Japan. *Suisan Gijutsu (J. Fish. Technol.)*, **1**, 39-44 [In Japanese with English summary].

Ito, R. & Ogawa, H. (1999) Culture experiment of artificial juvenile of Manila clam, using net covering. *Oita-ken Kaiyo Suisan, Kenkyu Center Tyousa Kenkyu Houkoku*, **2**, 23-30 [In Japanese].

Izumikawa, K. et al. (2015) Effect of cover nets on survival of Manila clam *Ruditapes philippinarum* in an artificial tidal flat of Yori-shima in Asakuchi City. *Bull. Fish. Exp. Stn. Okayama Pref.*, **30**, 17-23 [In Japanese].

Japan Meteorological Agency (2019) *Sea surface temperature (around Japan)*. https://www.data.jma.go.jp/gmd/kaiyou/english/long_term_sst_japan/sea_surface_temperature_around_japan.html.

Kanazawa, T. (2003) The fishing distribution and food of the Japanese stingray (*Dasyatis akajei*) in the Ariake Sea of the water temperature descending term. *Bull. Fukuoka Fish.*

Mar. Technol. Res. Cent., **13**, 149-152 [In Japanese].

Kimura, H. (2005) Predator–prey relationship between crabs and short-necked clam, *Ruditapes philippinarum*. *Bull. Yamaguchi Pref. Fish. Res. Ctr.,* **3**, 97-103 [In Japanese with English summary].

Kodama, O. & Taino, S. (2014) Stock recovery experiments for the asari clam. *H.26 Nendo Kochi-ken Suisan Shikenjyo Jigyo Houkokusho*, **112**, 118-134 [In Japanese].

Kumagai, N. H. et al. (2018) Ocean currents and herbivory drive macroalgae-to-coral community shift under climate warming. *Proc. Natl. Acad. Sci. USA*, **115**, 8990-8995.

Lewis, T. L. et al. (2007) Effects of predation by sea ducks on clam abundance in soft-bottom intertidal habitats. *Mar. Ecol. Prog. Ser.*, **329**, 131-144.

Mallet, D. & Pelletier, D. (2014) Underwater video techniques for observing coastal marine biodiversity: a review of sixty years of publications (1952-2012). *Fish. Res.*, **154**, 44-62.

Ochiai, A. & Tanaka, M. (1986) *Ichthyology II*. Kouseisha-kouseikaku, Tokyo [In Japanese].

Okamoto, K. (2000) Influence on little clam *Ruditapes philippinarum* stock by the predation of moon snail *Neverita didyma* in Lake Hamana. *Bull. Shizuoka Pref. Fish. Exp. Stn.*, **35**, 33-34 [In Japanese].

R Core Team (2019) *R: a language and environment for statistical computing.* R Foundation for Statistical Computing, Vienna, Austria. https://www.R-project.org/.

Saito, H. et al. (2010) Effect of cover nets on survival rate of clam released in Mitsu Bay, Hiroshima Prefecture. *Suisan Zoushoku*, **58**, 525-527 [In Japanese with English summary].

Sato, S. et al. (2012) Long-term fluctuations in mollusk populations before and after the appearance of the alien predator *Euspira fortunei* on the Tona coast, Miyagi Prefecture, northern Japan. *Fish. Sci.*, **78**, 589-595.

Segawa, N. & Hattori, K. (1997) Influence on short-necked clam stock by the predation of moon snail on Kosugaya tidal flat in Ise Bay. *Bull. Aichi Fish. Res. Inst.*, **4**, 41-48 [In Japanese with English summary].

Shibata, T. & Kawanishi, S. (1999) Outbreak, predation on Japanese little neck clam *Ruditapes philippinarum*, and removal of moon snail, *Neverita didyma*, on Banzu and Futtsu tidal flats in Tokyo Bay. *Bull. Chiba Pref. Fish. Exp. Sta.*, **55**, 25-31 [In Japanese].

Shigeta, T. & Usuki, H. (2012) Predation on the short-neck clam *Ruditapes philippinarum* by intertidal fishes: a list of fish predators. *Suisan Gijutsu (J. Fish. Technol.)*, **5**, 1-19 [In Japanese with English summary].

Siddiqui, S. A. et al. (2018) Automatic fish species classification in underwater videos: exploiting pre-trained deep neural network models to compensate for limited labelled data. *ICES J. Mar. Sci.*, **75**, 374-389.

Sun, Y. F. et al. (2017) Prey selection of the swimming crab *Portunus trituberculatus* (Miers, 1876) (Brachyura: Portunidae) foraging on bivalves. *J. Crustacean Biol.*, **37**, 521-528.

Suzuki, K. et al. (2018) Predatory characteristics of the red stingray *Dasyatis akajei* for the commercially important clams in the Hii River system. *Laguna*, **25**, 31-38 [In Japanese with English summary].

Taga, S. et al. (2005) Growth and survival of the short-necked clam *Ruditapes philippinarum* stocked on the tidal flats in

the Seto Inland Sea, Yamaguchi Prefecture. *Bull. Yamaguchi Pref. Fish. Res. Ctr.*, **3**, 87-96 [In Japanese with English summary].

Takada, Y. et al. (2020) Spatial hierarchical partitioning of macrobenthic diversity of clam (*Ruditapes*) fishing grounds over a large geographical range of Japan. *Ecol. Res.* https://doi.org/10.1111/1440-1703.12172.

Takahashi, K. et al. (2016) Predation mechanism of Japanese rock crab on Manila clam *Ruditapes philippinarum* with possible countermeasures. *Nippon Suisan Gakkaishi*, **82**, 706-711 [In Japanese with English summary].

Tamaki, A. et al. (2008) Spatial partitioning between species of the phytoplankton-feeding guild on an estuarine intertidal sand flat and its implication on habitat carrying capacity. *Est. Coast. Shelf Sci.*, **78**, 727-738.

Tezuka, N. et al. (2012) Settlement, mortality and growth of the asari clam (*Ruditapes philippinarum*) for a collapsed population on a tidal flat in Nakatsu, Japan. *J. Sea Res.*, **69**, 23-35.

Tezuka, N. et al. (2014) *Ruditapes philippinarum* mortality and growth under netting treatments in a population-collapsed habitat. *Coastal Ecosystems*, **1**, 1-13.

Tezuka, N. (2018) *Parapara viewer.* Administered by the National Research Institute of Fisheries and Environment of Inland Sea, Fisheries Research Agency, Hiroshima, Japan. http://feis.fra.affrc.go.jp/seika/tayousei/fishdiv/parapara_viewer.html.

Toba, M. et al. (2007) Observations on the maintenance mechanisms of metapopulations, with special reference to the early reproductive process of the Manila clam *Ruditapes philippinarum* (Adams & Reeve) in Tokyo Bay. *J. Shell. Res.*, **26**, 121-130.

Toba, M. (2017) Revisiting recent decades of conflicting discussions on the decrease of Asari clam *Ruditapes philippinarum* in Japan: a review. *Nippon Suisan Gakkaishi (J. Jpn. Soc. Fish. Sci.)*, **83**, 914-941 [In Japanese with English summary].

Toba, M. et al. (2020) Characteristic changes in the population dynamics of asari (Manila) clam *Ruditapes philippinarum* in a period of stock decrease on the Banzu intertidal flat, Tokyo Bay. *J. Sea Res.*, **157**, 101845.

Tsujino, M. & Shigeta, T. (2019) Influence of Asari clam (*Ruditapes philippinarum*) abundance increase caused by cover-net on the nematode assemblages on a tidal flat. *Jpn. J. Benthol.*, **74**, 25-34 [In Japanese with English summary].

Usuki, H. et al. (2012) Tank experiments for prevention of predation on short-neck clam *Ruditapes philippinarum* by longheaded eagle ray *Aetobatus flagellum*. *Suisan Gijutsu (J. Fish. Technol.)*, **5**, 57-66 [In Japanese with English summary].

Yamaguchi, A. et al. (2005) Occurrence, growth and food of longheaded eagle ray, *Aetobatus flagellum*, in Ariake Sound, Kyushu, Japan. *Environ. Biol. Fish.*, **74**, 229-238.